Aggregation of a Dibenzo[*b*,*def*]chrysene Based Organic Photovoltaic Material in Solution

Alexandr N. Simonov,[‡,*] *Peter Kemppinen,*[§] *Cristina Pozo-Gonzalo,*[‡] *John F. Boas,*[†] *Ante Bilic,*[††] *Andrew D. Scully,*[§] *Adel Attia,*[‡] *Ayman Nafady,*[‡] *Elena A. Mashkina,*[‡] *Kevin N. Winzenberg,*[§] *Scott E. Watkins,*[§,*] *Alan M. Bond*[‡,*]

[‡] School of Chemistry, Monash University, Clayton, Victoria, 3800, Australia

[§] CSIRO Materials Science and Engineering, Private Bag 33, Clayton South, Victoria 3169, Australia

[†] School of Physics, Monash University, Clayton, Victoria, 3800, Australia

[††] CSIRO Computational Informatics, Private Bag 33, Clayton South, Victoria, 3169, Australia

ABSTRACT. Detailed electrochemical studies have been undertaken on molecular aggregation of the organic semiconductor 7,14-bis((triisopropylsilyl)-ethynyl)dibenzo[*b,def*]chrysene (TIPS-DBC), which is used as an electron donor material in organic solar cells. Intermolecular association of neutral TIPS-DBC molecules was established using ^{1}H NMR spectroscopy as well as by the pronounced dependence of the colour of TIPS-DBC solutions on concentration. Diffusion limited current data provided by near steady-state voltammetry also reveal aggregation. Furthermore, variation of concentration produces large changes in shapes of transient DC and Fourier transformed AC (FTAC) voltammograms for oxidation of TIPS-DBC in dichloromethane. Subtle effects of molecular aggregation on the reduction of TIPS-DBC are also revealed by the highly sensitive FTAC voltammetric method. Simulations of FTAC voltammetric data provide estimates of the kinetic parameters associated with oxidation and reduction of TIPS-DBC. Significantly, aggregation of TIPS-DBC facilitates both one-electron oxidation and reduction by shifting the reversible potentials to less and more positive values, respectively. EPR spectroscopy is used to establish the identity of one-electron oxidized and reduced forms of TIPS-DBC. Implications of molecular aggregation on the HOMO energy level in solution are considered with respect to efficiency of organic photovoltaic devices utilising TIPS-DBC as an electron donor material.

KEYWORDS: AC and DC voltammetry; simulations; NMR; HOMO energy level; π-π stacking.

INTRODUCTION

Since the first reports of significant power conversion efficiencies available with organic photovoltaic (OPVs)[1] cells there has been sustained interest in the development of new materials and device architectures with the aim of delivering on the promise of low cost, light-weight, solar power. In recent years, the nature of the compounds used as the electron donor in solution processed, bulk heterojunction devices has expanded from conjugated polymers to also include solubilised small molecules.[2,3] One of the key parameters used for selecting materials for OPVs are the molecular energy levels. Apart from factors such as electrode materials, light intensity and temperature of operation, the device open circuit voltage (V_{oc}) has been shown to be proportional to the donor/acceptor energy gap (ΔE_{DA}), *i.e.* the difference between the energies of the highest occupied molecular orbital (HOMO) of the donor and the lowest unoccupied molecular orbital (LUMO) of the acceptor. The correlation between the V_{oc} and ΔE_{DA} has been recognized experimentally for different types of OPVs[4-6] and linearity of the V_{oc} - ΔE_{DA} dependence has been rationalized theoretically.[7]

In order to produce a functional OPV device, the combination of an electron donor and an electron acceptor must satisfy a number of key criteria. Firstly, the LUMO of the acceptor and the LUMO of the donor must be sufficiently offset to facilitate charge separation. Next, the HOMO of the donor and the LUMO of the acceptor must be appropriately aligned with the respective electrodes to enable collection of charges. Finally, the ΔE_{DA} should be as large as possible to maximise the V_{oc} of the OPV. Satisfying these criteria clearly relies on accurate measurements of all of the energy levels.

In the solid state (thin films) the HOMO energies of materials can be directly estimated by a number of techniques such as ultra-violet photoemission spectroscopy (UPS),[8,9] photoelectron

spectroscopy in air (PESA) and Kelvin Probe analyses.[10] These techniques directly probe removal of an electron from a populated state in a material. By contrast, measurement of an unfilled state, the LUMO, is considerably more difficult. While some information can be obtained from UV-visible absorption (UV-Vis) spectroscopy and inverse photo electron spectroscopy (IPES),[11] solution-based measurements using cyclic voltammetry remain popular due to the relatively simple experimental requirements.[12,13]

The use of cyclic voltammetry as a technique for estimating the HOMO and LUMO energy levels of materials is sound, in theory, but in practice there have been very few thorough electrochemical studies in the area of organic electronics. For polymers, the use of solution-based measurements is complicated by slow mass-transport kinetics of large molecules. The use of thin films is also difficult, as ions must move in and out of a film thus introducing a kinetic component to the required thermodynamic measurement. For small semiconducting molecules in solution, a detailed study of the electrochemical properties and hence provision of detailed knowledge related to the redox chemistry of a material is possible and is a task that we have undertaken in this report. To our knowledge the potentially complicating effects of molecular aggregation on the electrochemistry of these systems has largely been ignored.

The small-molecule organic semiconductor we have chosen to study in detail in this paper is the polycyclic aromatic compound, 7,14-bis((triisopropylsilyl)-ethynyl)dibenzo[*b*,*def*]chrysene (TIPS-DBC, Chart 1). When first reported, TIPS-DBC produced OPVs displaying a benchmark power conversion efficiency for solution processed small molecules.[14] More recently, it has been shown that this compound is somewhat special in being processable into OPV devices by either solution or vacuum deposition methods.[15] A detailed study of this compound showed that the V_{oc} values predicted on the basis of ΔE_{DA} and those obtained experimentally might differ due to the

dependence of V_{oc} on other parameters determined by the electronic properties of the donor/acceptor system. The TIPS-DBC based devices demonstrate a remarkable dependence on the intraphase microstructure of the donor layer, which has been found to determine bulk hole mobility, mean exciton diffusion length, charge carrier generation efficiency, recombination rate and the HOMO level of the donor.[15] Intermolecular association of TIPS-DBC molecules in the donor layer has been conjectured as being the origin of the observed differences. PESA studies revealed a 0.08 eV difference in the HOMO levels for different morphologies of TIPS-DBC donor layers.[15]

Chart 1. (a) TIPS-DBC and (b) putative structure of π-π stacked TIPS-DBC dimer.

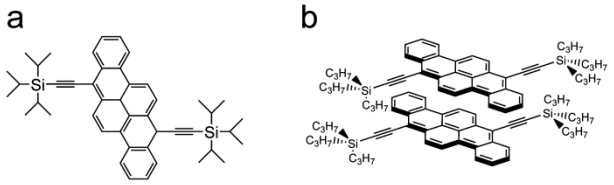

As noted above, experimental quantification of the HOMO/LUMO levels of the redox active species can be achieved using conventional DC cyclic voltammetry, as reported for TIPS-DBC in dichloromethane in a preliminary communication on dibenzo[*b*,*def*]chrysene based semiconductors.[14] An important advantage provided by voltammetric analysis is the possibility of establishing the influence of molecular aggregation on the energy levels *via* undertaking measurements at variable concentration. This virtue has not been exploited to date and forms the basis for the present study which is aimed at revealing the impact of molecular aggregation on the energy levels and redox chemistry of TIPS-DBC. The concentration dependent electrochemistry of TIPS-DBC is probed by a set of electrochemical techniques that include the very sensitive Fourier transformed AC voltammetric (FTACV) method[16] in conjunction with NMR, EPR and UV-Vis spectroscopic characterization of neutral, oxidized and reduced species in

dichloromethane. To establish the correlation between the properties of organic semiconductor in solution and in the solid-state, the HOMO energy level data derived from the voltammetric studies on dissolved TIPS-DBC are compared to those available from the characterization of the evaporated and spin-coated TIPS-DBC films.

EXPERIMENTAL

Materials. Tetra(*n*-butyl)ammonium hexafluorophosphate ((*n*-Bu)$_4$NPF$_6$; 98%, Wako) used as the supporting electrolyte in electrochemical experiments was recrystallized twice from ethanol (96%, Merck Emplura). Tetra(*n*-Butyl)ammonium *tetrakis*(perfluorophenyl)borate ((*n*-Bu)$_4$N-B(C$_6$F$_5$)$_4$) was synthesized according to a literature procedure.[17] Ferrocene (Fc; 98%, Ega-Chemie), acetone (≥99.0 %, Merck Emplura), acetonitrile (≥99.9%, Merck LiChrosolv) and CD_2Cl_2 (99.9%; Cambridge Isotope Laboratories Inc.) were used as supplied. Dichloromethane (≥99.9%, MERCK Suprasolv) was distilled over CaH_2 under a N_2 atmosphere prior to use. High-purity nitrogen (99.999 %, H_2O < 3 ppm, O_2 < 2 ppm) was used in experiments requiring removal of oxygen. High-purity water used in this study was obtained from an Arium 61315 (Sartorius) water purification system.

TIPS-DBC was synthesized according to the procedure described in Ref.[14] The purity was determined to be 96 mol. % by high-performance liquid chromatography (HPLC) (Fig. S1, Supporting Information).

Electrochemical instrumentation and procedures. Electrochemical experiments were performed in three-electrode cells at ambient temperature (296-298 K) under a high purity N_2 atmosphere using either an Epsilon Electrochemical Workstation (BAS) or a custom-made FTACV instrument.[16] The working electrodes were a glassy carbon (GC, diameter 1 or 3 mm)

macrodisk or a carbon fibre microelectrode (diameter 12 μm) which were treated using the standard procedures described in Supporting Information. Controlled potential electrolysis experiments were performed in a three compartment cell with fine porosity glass frits separating the chambers using platinum gauze as working electrode under ambient laboratory conditions (oxidation only) or inside a nitrogen-filled glove-box (both oxidation and reduction) (see Supporting Information for details). Potentials are reported *versus* the formal reversible potential of the $Fc^{0/+}$ couple, as measured in the same solution. Unless otherwise stated, current data are normalized to the electrode surface area.

Other procedures. Characterization of TIPS-DBC before and after one-electron reduction or oxidation was performed using HPLC along with ^{1}H NMR, UV-Vis-NIR and EPR spectroscopy as appropriate and as described in Supporting Information.

Simulations of the DC and AC cyclic voltammetry were undertaken using DigiElch-Professional 7.F[18] and Monash Electrochemistry Simulator[19] software packages, respectively, using the Butler-Volmer formalism to provide a description of the charge-transfer kinetics:

$$I = F \cdot A \cdot k^0 \cdot \left(C_{x=0}^{Red}(t) \cdot \exp\left((1-\alpha) \cdot \frac{F\left(E - E^0\right)}{RT} \right) - C_{x=0}^{Ox}(t) \cdot \exp\left(-\alpha \cdot \frac{F\left(E - E^0\right)}{RT} \right) \right),$$

where $F = 96485$ / $C\ mol^{-1}$ is the Faraday constant; A / cm^2 is the surface area of the electrode, k^0 / $cm\ s^{-1}$ is the heterogeneous charge transfer rate constant; $C_{x=0}^{Red}(t)$ and $C_{x=0}^{Ox}(t)$ / $mol\ cm^{-3}$ are the concentrations of reduced and oxidized forms of electractive species at the working electrode surface (where x, the distance from the surface, is zero) as a function of time (t / s); α is the charge transfer coefficient assumed in all simulations to be 0.50; E / V is the true potential of the electrode and E^0 / V is the formal potential of the redox couple relative to a reference couple.

Density Functional Theory (DFT) calculations were carried out using a Gaussian 09 suite of programs[20] as described in Supporting Information.

RESULTS AND DISCUSSION

Aggregation of TIPS-DBC molecules in solution. Prior to undertaking voltammetric studies on TIPS-DBC, the chemical nature of the species present in solution needs to be established. The first clue for concentration dependence of the species present in dichloromethane was provided by visual inspection of the colour of the solutions as a function of total TIPS-DBC concentration (C_{TD}). On decreasing the concentration, apart from the obvious diminution of the intensity, the colour changes from rich red to peach and then to yellow-green (Fig. 1).

Figure 1. Photograph showing the colours of dichloromethane solutions as a function of TIPS-DBC concentration (from left to right: 10, 5, 2.5, 1.25, 0.125 mM).

The UV-Vis spectrum of a TIPS-DBC solution having a relatively low concentration (*ca* 6 μM) exhibits five main absorption bands with maximum absorbance (λ_{max}) at 317, 332, 444, 476 and 510 nm (Fig. 2a). The λ_{max} values for the most intense absorption bands at 317, 332 and 510 nm are in good agreement with the theoretical prediction of 3 prominent singlet-singlet transitions at 318, 335 and 546 nm (see Fig. 2a and Supporting Information, Table S1). Two other allowed singlet transitions calculated to occur at 408 and 326 nm have oscillator strengths close to zero. Thus, for the values of C_{TD} in the μM range, dichloromethane solutions of TIPS-DBC appear to comprise essentially individual un-associated molecules, whereas the effects of aggregation are evident at the mM-level concentrations relevant to Fig. 1. The very high extinction coefficients for TIPS-DBC in dichloromethane ($8.80 \cdot 10^4$ and $1.28 \cdot 10^5$ M^{-1} cm^{-1} at λ = 510 and 332 nm, respectively) require much narrower optical path lengths than were available to us for recording

UV-Vis spectra of the solutions shown in Fig. 1. As a result, we were unable to obtain details of solute aggregation by UV-Vis spectroscopy.

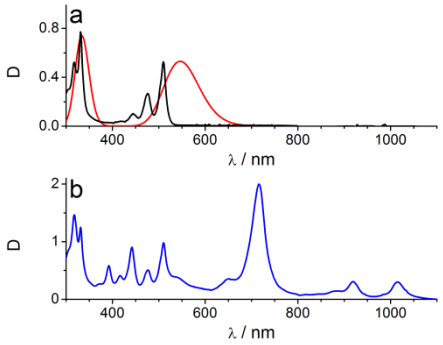

Figure 2. UV-Vis-NIR absorption spectra of a dilute solution of TIPS-DBC (C_{TD} *ca* 6 μM) in CH_2Cl_2 (0.2 M (*n*-Bu)$_4$NPF$_6$) (a) before and (b) after bulk oxidative electrolysis at 0.81 V *vs.* $Fc^{0/+}$. Panel (a) also shows the theoretically calculated spectrum for neutral TIPS-DBC (*red*).

The environment-sensitive technique ^{1}H-NMR spectroscopy confirms that concentration dependent structural changes take place in CD_2Cl_2 solutions of TIPS-DBC when C_{TD} is varied over the range relevant to Fig. 1. An estimate of the equilibrium constant for the aggregation of TIPS-DBC molecules can be obtained from the analysis of the shift of the ^{1}H-NMR resonances as a function of C_{TD} (Fig. 3).

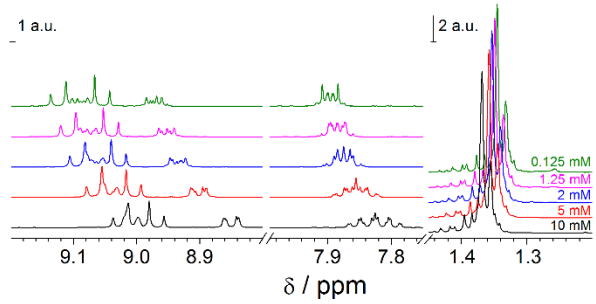

Figure 3. ^{1}H NMR spectra of TIPS-DBC in CD_2Cl_2 as a function of concentration: 10 mM (*black*), 5 mM (*red*), 2 mM (*blue*), 1.25 mM (*magenta*) and 0.125 mM (*green*). Note that the ordinate scales for the 9.20-7.75 ppm and 1.50-1.20 ppm regions differ by a factor of 2. For assignment of resonances see Ref.[14]

For simplicity, the aggregated form of TIPS-DBC extant over the concentration range used in the present work is assumed to be a slipped π-π stacked "dimer" (reaction **I** and Chart 1b) having an inter-stack separation distance of 3.2 Å and a slippage angle along the long molecular axis of 25º, based on the one-dimensional head-to-tail slipped-stack arrangement reported for the crystalline material.[21] The association constant for the "dimer", K^{SS} (*S*-*S* stands for the 'substrate-substrate'), is defined by equation 1.

$$\left[TIPS\text{-}DBC\right]^0 + \left[TIPS\text{-}DBC\right]^0 \underset{}{\overset{K^{SS},k_f^{SS}}{\rightleftharpoons}} \left[TIPS\text{-}DBC\cdots TIPS\text{-}DBC\right]^0 \quad \textbf{I}$$

where k_f^{SS} / M^{-1} s^{-1} is the rate constant of the forward bimolecular reaction.

$$K^{SS} = \frac{C_D}{\left(C_{TD} - 2\cdot C_D\right)^2} \quad (1)$$

On this basis, C_D is the concentration of the "dimer" [TIPS-DBC···TIPS-DBC]^0 considered to be formed as a consequence of the equilibrium constant K^{SS} and total concentration of TIPS-DBC molecules, C_{TD}. Of course, it is possible that aggregation is more extensive (N-mer) than "dimerization", and appropriate methods for analysis of the NMR data taking into account formation of N-mers have been developed.[22,23] However, more extensive aggregation was not considered in analysis of the NMR data for TIPS-DBC since electrochemical data suggest that this is not significant (*vide infra*).

In the following analysis, based on the simplest case of aggregation by "dimerization", it is assumed that the ^{1}H NMR spectrum for the lowest 0.125 mM concentration available (see Fig. 3) corresponds to that of the TIPS-DBC monomer. Theoretically, the π-π stacking model assumed for aggregation of TIPS-DBC molecules having modestly sized π-system is unlikely to provide a large K^{SS} value in low polarity solvents such as dichloromethane used in this work.[24] Moreover, as will be shown below by analysis of the near steady-state voltammetric data, the K^{SS} value does not

exceed $2 \cdot 10^2$ M^{-1}, which corresponds to less than 5 % degree of "dimerization" of TIPS-DBC at C_{TD} = 0.125 mM. It is also assumed that the rate of dimerization is fast on the NMR timescale and this is supported by results from simulations of the electrochemical data presented below. Use of these assumptions allows the ^{1}H NMR data to be analysed in terms of time averaged spectra derived from a monomer and a "dimer". On this basis, the experimentally observed chemical shifts, δ_{Obs}, can be expressed as a weighted average of the chemical shifts associated with the monomer and "dimer", δ_D and δ_M, respectively:

$$\delta_{Obs} = \frac{2 \cdot C_D}{C_{TD}} \cdot \delta_D + \frac{C_{TD} - 2 \cdot C_D}{C_{TD}} \cdot \delta_M \quad . \tag{2}$$

After expression of C_D in terms of K^{SS} and C_{TD} and some algebra provided in the Supporting Information, equations 1 and 2 can be rearranged to give an expression for the dependence of $\Delta\delta_{Obs} = \delta_{Obs} - \delta_M$ on C_{TD} as given in equation 3.

$$\frac{C_{TD}}{\Delta\delta_{Obs}} = \frac{2}{\delta_D - \delta_M} \cdot \left(C_{TD} - C_D\right) + \frac{1}{K^{SS}} \cdot \frac{1}{2 \cdot \left(\delta_D - \delta_M\right)} \quad . \tag{3}$$

Although K^{SS}, δ_D and C_D are unknown, a combination of graphical and iterative procedures can be used to determine K^{SS}. If $C_D << C_{TD}$, equation 3 can be simplified to give a linear relationship between $\Delta\delta_{Obs}^{-1}$ and C_{TD}^{-1} with an intercept of $2 \cdot (\delta_D - \delta_M)^{-1}$ and a slope of $(2 \cdot K^{SS} \cdot (\delta_D - \delta_M))^{-1}$, which provided an initial estimate of K^{SS}. The $\Delta\delta_{Obs}$ data derived from the ^{1}H NMR signal with the highest chemical shift was used in these calculations. The K^{SS} value was then refined using an iterative procedure[25] to fit equations 2 and 3 to the experimental ^{1}H NMR data obtained from the solutions of TIPS-DBC and was finally estimated as *ca* 10 M^{-1}. An almost identical K^{SS} value is recovered by applying non-linear least squares analysis to the experimental $\Delta\delta_{Obs}(C_{TD})$ data set. As already mentioned, further aggregation of TIPS-DBC is of course probable, but is neglected in the analysis.

DC cyclic voltammetry of TIPS-DBC in dichloromethane. Preliminary cyclic voltammetric studies by Winzenberg et al.[14] revealed that TIPS-DBC undergoes one reduction and one oxidation process in dichloromethane solution containing $(n\text{-Bu})_4NPF_6$ as the supporting electrolyte. Based on analysis of classical criteria of peak-to-peak separation for the oxidation and reduction peak potentials (ΔE_p), the reduction process was suggested to be reversible ($\Delta E_p \approx 0.08$ V as also found for the known reversible $Fc^{0/+}$ process under the same conditions) while the oxidation was assigned as quasi-reversible ($\Delta E_p \approx 0.18$ V). However, since the TIPS-DBC molecules "dimerize", the voltammetric results are not expected to be fully explained by simple one-electron transfer events involving individual monomers only. The key experiment in cyclic voltammetry needed to check for effects of aggregation is the concentration dependence, which was not established in the initial report.[14]

To establish if "dimerization" contributes to electrooxidation and electroreduction of TIPS-DBC, as should be the case according to the above analysis of the NMR data, the voltammetry was studied over the similar concentration range as that used to obtain the NMR data. DC and AC cyclic voltammetric experiments were undertaken at both macro and microdisk electrodes along with the spectroscopic characterization of the reduction and oxidation products.

Within the potential range -2.0 – +1.0 V and under conditions of DC cyclic voltammetry TIPS-DBC exhibits one reduction and one oxidation process separated by *ca* 2.2-2.3 V (Fig. 4), consistent with the previous findings.[14] Minor processes detected prior to the main reduction process (see inset in Fig. 4a) are attributed to the presence of trace impurities, that were identified in the batch of TIPS-DBC used in this study (Fig. S1, Supporting Information). As reported previously,[14] ΔE_p values for the first reduction process for TIPS-DBC (Fig. 4a) are only slightly higher than predicted for a simple reversible one-electron process. For example, ΔE_p values of

0.091 and 0.069 V were obtained for the reduction of 1 and 0.24 mM TIPS-DBC dichloromethane solutions, respectively, at v = 0.10 V s^{-1}. However, since the uncompensated resistance is R_u = 450-410 Ω, most of this difference from above 0.060 V expected theoretically for a simple one-electron process is essentially explicable in terms of (Ohmic) IR_u drop.

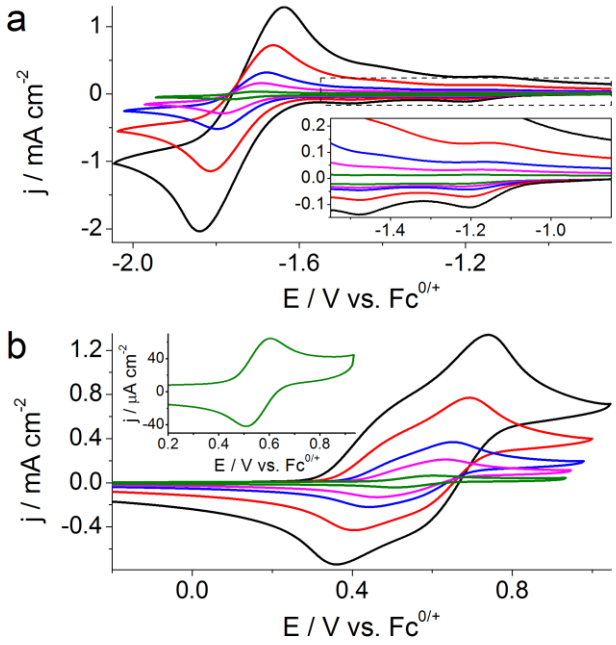

Figure 4. DC cyclic voltammograms obtained at a scan rate of 0.10 V s^{-1} with a GC electrode for (a) reduction and (b) oxidation of TIPS-DBC in CH_2Cl_2 (0.2 M (n-Bu)$_4$NPF$_6$) as a function of concentration: 10 (*black*), 5 (*red*), 2 (*blue*), 1 (*magenta*) and 0.24 mM (*green*). Insets show expanded plots of region (a) outlined with a dashed box and (b) for 0.24 mM data.

Apart from the IR_u induced increase in ΔE_p, an increase in concentration of TIPS-DBC does not cause other notable changes in the DC cyclic voltammetric profile for this first reduction process (Fig. 4a). In contrast, the cyclic voltammetry for the first oxidation process displays a remarkably strong dependence on C_{TD}. As demonstrated in Fig. 4b, increasing the concentration of TIPS-DBC induces the transformation from a shape resembling that of a reversible one-electron process, to a much more complicated profile consisting of (at least) two unresolved processes. This strong

concentration dependence qualitatively resembles the peculiarities reported for redox transformations proceeding *via* a *r*adical-substrate (RS) dimerization mechanism as described by Geiger *et al.*[17,26] However, the electrochemistry of TIPS-DBC must be different from these RS schemes since "dimerization" is known to occur prior to electron transfer. Closely related aggregation mechanisms apply to the electrochemistry of dyes and other planar molecules with a high degree of conjugation.[27-29]

Examination of cyclic voltammograms over a wider potential range reveals the capacity of TIPS-DBC to undergo further oxidation and reduction in dichloromethane (Fig. 5). The second oxidation process has a mid-point potential (average of oxidation and reduction peak potentials) of 1.20 V and is chemically reversible when a tetrabutylammonium salt of the weakly-coordinating anion, $(n\text{-Bu})_4NB(C_6F_5)_4$, is employed as the supporting electrolyte. However, the process is chemically irreversible in the presence of $(n\text{-Bu})_4NPF_6$ as the supporting electrolyte. The second TIPS-DBC reduction step is chemically irreversible and has a reduction peak potential E_p^{Red} of -2.2 – -2.3 V with a scan rate of 0.10 V s^{-1}. In general, it is only the first oxidation and reduction processes that are used to estimate HOMO and LUMO energy levels for use in OPV device design. As such, the second oxidative and reductive electrochemical processes were not studied in detail, although, the electrolyte dependence is noteworthy.

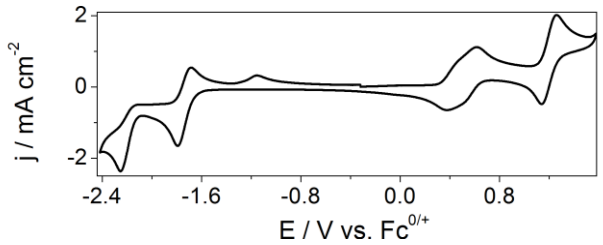

Figure 5. Cyclic voltammogram obtained at a scan rate of 0.10 V s^{-1} with a GC electrode over a wide potential range for 7.5 mM TIPS-DBC in dichloromethane (0.1 M $(n\text{-Bu})_4NB(C_6F_5)_4$) under glove-box conditions.

Steady state voltammetry of TIPS-DBC in dichloromethane. Near steady-state voltammetry exhibited by TIPS-DBC at a microelectrode reveals only small differences in the magnitudes of limiting current values for oxidation and reduction. Thus, the number of electrons transferred in each step are assumed to be identical (Fig. 6a). As confirmed by coulometric analysis of bulk electrolysis data (see below), the processes involve one-electron oxidation and reduction of TIPS-DBC.

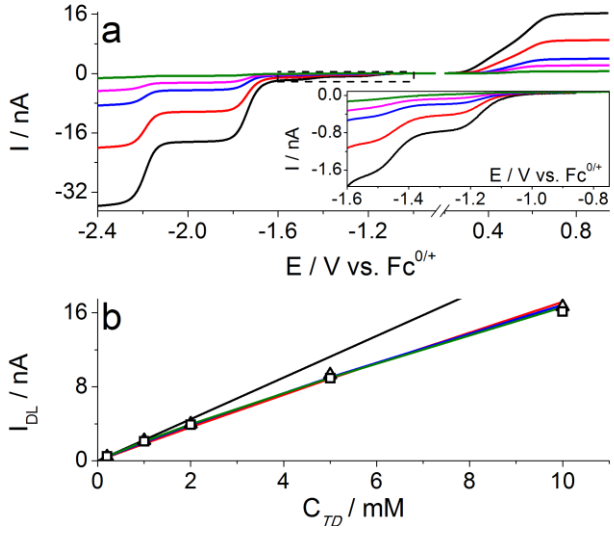

Figure 6. (a) Near steady-state voltammograms (ν = 0.01 V s^{-1}) obtained with a carbon fibre microelectrode (diameter 12 μm) for reduction and oxidation of TIPS-DBC in CH_2Cl_2 (0.2 M (*n*-Bu)$_4$NPF$_6$) at concentrations of: 10 (*black*), 5 (*red*), 2 (*blue*), 1 (*magenta*) and 0.24 mM (*green*). Inset shows an expanded version of the region in the dashed box. (b) Diffusion limited currents (I_{DL}) obtained from one-electron reduction (Δ) and oxidation (□) of TIPS-DBC as a function of the total concentration of TIPS-DBC and theoretical I_{DL} values calculated for K^{SS} = 150 (*green*), 50 (*blue*) and 10 M^{-1} (*red*) (see text for details). The *black* line is the linear plot extrapolated from low concentration data.

Non-linear plots of diffusion limited currents measured at a microelectrode (I_{DL}) as a function of concentration of TIPS-DBC provide further evidence of the complexity of the electrode process (Fig. 6b). Use of the relationship $I_{DL} = 4 \cdot n \cdot F \cdot r \cdot C_{TD} \cdot D$ (where n is the number of transferred electrons, r is the microdisk electrode radius, D is the diffusion coefficient of electroactive species) implies that the diffusion coefficient decreases upon increasing the concentration of TIPS-DBC. This is as expected when "dimer" formation occurs at high concentrations, as a higher molecular weight "dimer" will diffuse more slowly than the monomer.

The dependence of I_{DL} on C_{TD} may be interpreted in terms of the diffusion of both TIPS-DBC monomers and [TIPS-DBC···TIPS-DBC] "dimers" with their electrochemical transformations probably involving 1 and 2 electrons, respectively. Taking into account the stoichiometry of reaction **I**, I_{DL} values can be expressed as:

$$I_{DL} = 4 \cdot F \cdot r \cdot \left(2 \cdot D_D \cdot C_D + 1 \cdot D_M \cdot \left(C_{TD} - 2 \cdot C_D\right)\right), \quad (4)$$

where D_M and D_D are diffusion coefficients of the monomer and "dimer", respectively, although again it is noted that "dimerization" is used here as the simplest case of molecular aggregation.

According to the Stokes-Einstein equation, which advises that $D \propto R^{-1}$ (where R is the radius of diffusing species), the diffusion coefficient for the "dimer" might be expected to be approximately one-half that of the monomer. On this basis we can write

$$D_D = 0.5 \cdot D_M. \quad (5)$$

On the basis of calculation of C_D from K^{SS} and C_{TD}, equation 4 can then be rearranged (see Supporting Information) to give:

$$I_{DL} = D_M \cdot F \cdot r \cdot \left[2 \cdot C_{TD} - \frac{1}{2 \cdot K_{SS}} + \sqrt{\frac{1}{4 \cdot K_{SS}^{\,2}} + \frac{2 \cdot C_{TD}}{K_{SS}}}\right]. \quad (6)$$

Correct values of D_M and K^{SS} should fit equation 6 for all concentrations C_{TD} and their corresponding limiting currents I_{DL}. In an attempt to estimate the ideal combination of the sought-for D_M and K^{SS} parameters, a standard deviation (SD_D) was computed as a function of K^{SS} for the set of 5 diffusion coefficients calculated using equation 6 and the experimental data presented in Fig. 6b. Within the range of the "dimerization" equilibrium constants between 0 and 10^4 M^{-1}, the $SD_D(K^{SS})$ dependence demonstrates a single minimum at $K^{SS} \approx$ 50-200 M^{-1}. Similarly, fitting the experimental $I_{DL}(C_{TD})$ data using non-linear least squares analysis yields a K^{SS} value of $1.5 \cdot 10^2 \pm 0.7 \cdot 10^2$ M^{-1}. The K^{SS} constant estimated on the basis of the $I_{DL}(C_{TD})$ dependence is greater than the value of 10 M^{-1} deduced from the NMR data, though it is noted that I_{DL} values computed using equation 4 are not very sensitive to K^{SS} (Fig. 6b). Plausibly, NMR might predominantly probe nearest neighbours and not be very sensitive to the formation of larger aggregates. Additionally, it is noted that electrochemical studies were performed with 0.2 M electrolyte present, which was absent in NMR studies. Thus, due to uncertainties in equation 5 and treatment of aggregation as a "dimerization" process, the K^{SS} value can only be estimated to lie in the range of 10 to 150 M^{-1}.

Spectroscopic analysis of the products of one-electron oxidation and reduction of TIPS-DBC. A dichloromethane solution containing 1 mM TIPS-DBC showed no EPR signal at room temperature (290 K) or at 77 K. Following one-electron bulk reductive electrolysis of 1 mM TIPS-DBC in dichloromethane at *ca* -1.9 V, the deep violet colour solution exhibited a strong EPR signal at 290 K with $g = 2.00273$ as shown in Figure 7. A simulated spectrum, based on the simplifying assumption that the unpaired electron interacts equally with four equivalent protons with a hyperfine interaction constant of *ca.* $1.7 \cdot 10^{-4}$ cm^{-1}, is also shown in Figure 7.

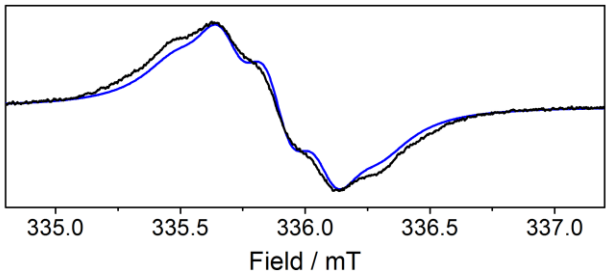

Figure 7. Experimental EPR spectrum at 290 K derived from reduction of 1 mM TIPS-DBC in dichloromethane (0.2 M (n-Bu)$_4$NPF$_6$) by controlled potential electrolysis at -1.9 V (*black*) and simulated EPR spectrum (*blue*) (see text and Supporting Information, Table S2 for the simulation parameters). Spectrometer settings: microwave frequency 9.415 GHz; microwave power 0.209 mW; receiver gain $1.0 \cdot 10^5$; 100 kHz modulation amplitude 0.05 mT; field scan range/time 4 mT/41.9 s; time constant 41 ms.

During the course of oxidative bulk electrolysis at 0.81 V, the orange colour of a 5 mM solution of TIPS-DBC in dichloromethane changed to dark green and finally to dark purple when oxidation was complete. When diluted to the μM level the UV-Vis-NIR spectrum differed significantly from that of the neutral compound at a similar concentration with the most intense band now being located at 715 nm (Fig. 2). A 1 mM solution, subjected to partial oxidative electrolysis at *ca.* 0.81 V under ambient conditions, was pale yellow in colour and exhibited a weak EPR signal at g ~ 2.0026. A poorly resolved 5-line hyperfine structure could be discerned from this solution phase spectrum, with a splitting of around $1.7 \cdot 10^{-4}$ cm^{-1} (Fig. S2, Supporting Information). A 1 mM TIPS-DBC solution subjected to exhaustive oxidative electrolysis was dark green in colour and exhibited a strong EPR signal at g = 2.00258 (± 0.000 15) at 290 K. This resonance showed less well resolved hyperfine structure than was observed for the yellow solution.

The difference in the g-values of the species in solutions after oxidative and reductive electrolysis is consistent with the resonances being due to radical cation and radical anion species

respectively. Although the absolute magnitudes of the *g*-values themselves are estimated to have uncertainties of around ± 0.000 15, the difference between those of the cation (2.002 58) and the anion (2.002 73) is experimentally significant. The relative values, with $g_{anion} > g_{cation}$ are in accord with expectation for the contribution to the *g*-values *via* spin-orbit coupling from filled (anion) and empty (cation) molecular orbitals.[30]

Information about the distribution of electron density over the anion and cation is in principle obtainable from analysis of the hyperfine structure. In many cases, the spectra of similar radicals in solution exhibit complex and well-resolved multiline spectra as a consequence of the tumble averaging of anisotropic interactions. In the present case, the spectra are only poorly resolved, most likely because of insufficient tumble averaging. Although the spectra can be simulated as shown in Figures 7 and S2 by assuming a hyperfine interaction of magnitude $1.7 \cdot 10^{-4}$ cm^{-1} with four equivalent protons, a calculation of the spin densities (not shown) indicates that this interpretation is an over-simplification as the unpaired electron is highly delocalised over the entire molecular framework. More completely resolved spectra would be required to resolve this issue.

The EPR spectra recorded at very high spectrometer gain settings and over the magnetic field range from 5 mT up to $g \sim 2$ (336 mT), specifically in the region around $g \sim 4$ at 168 mT, showed no resonances other than those shown in Figures 7, S2 and S3 (Supporting Information). There is therefore no direct evidence for specific inter- or intra- molecular electron exchange or dipole-dipole interactions either in the liquid phase at 290 K or in frozen solution at 120 K at C_{TD} = 1 mM that could occur as a result of specific dimer formation by two anions or cations.

Fourier transformed AC voltammetry of TIPS-DBC in dichloromethane. In order to gain a deeper insight into the nature of the reduction and oxidation of TIPS-DBC in the -2.6 – 0.85 V potential range, the mechanistically sensitive FTACV method was employed. AC voltammetry

provides enhancement in the quality and quantity of information obtained per experiment, improvement in the separation of faradaic and non-faradaic components, facilitates deciphering of complexities in electrode mechanisms and increases the reliability of quantification of fast heterogeneous and homogeneous kinetics.[16,31] The aperiodic DC component and AC harmonics derived by applying the usual FFT/inverse-FFT sequence for the first reduction process are illustrated in Fig. 8 for a low and a high concentration of TIPS-DBC in dichloromethane (0.2 M (n-Bu)$_4$NPF$_6$). The contribution of the signals arising from the abovementioned trace impurities overlap in some of the harmonics, particularly at high C_{TD} (see *magenta* regions on the experimental curves in Fig. 8) Nevertheless, careful analysis of the harmonics still allows clear distinction to be made between the signals of interest and those produced by the impurities.

As evidenced by the equivalence of the current magnitudes in the harmonics derived from negative and positive potential direction sweeps in the FTAC cyclic voltammograms (Fig. 8), the first reduction step for TIPS-DBC is close to chemically reversible. The shapes of the AC harmonics measured for the dilute concentration of 0.24 mM, where only a minor contribution is expected from "dimerization", correspond closely to those expected for a simple one-electron process (*cf.* Fig. 8a and Figs. 1-5 of Ref.[32]). Nevertheless, even at this low concentration, a small departure from the ideal reversible shape of the harmonics (designated by dashed lines in Fig. 8a) is revealed.

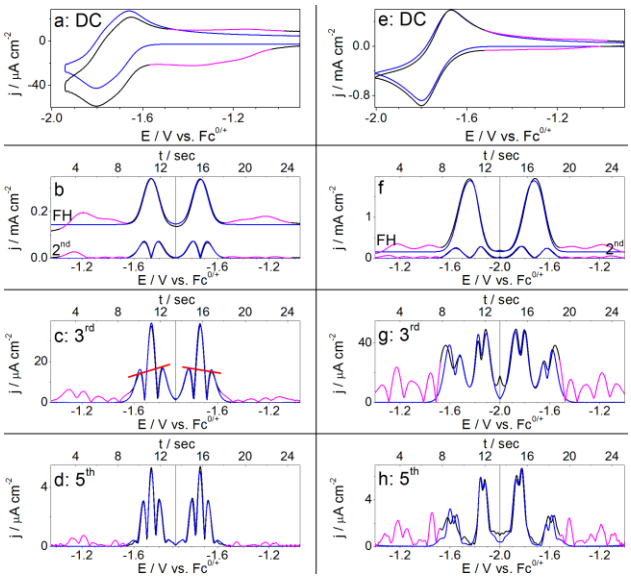

Figure 8. Aperiodic DC (a and e), AC fundamental (FH) and 2nd (b and f), 3rd (c and g) and 5th (d and h) harmonic components derived from FTAC voltammograms for reduction of (a-d) 0.24 and (e-h) 5 mM TIPS-DBC in CH_2Cl_2 (0.2 M $(n\text{-Bu})_4NPF_6$) at a GC electrode (*black* + *magenta*) and simulated data (*blue*). Dashed lines highlight non-ideality relative to a simple redox process. Experimental parameters: $\upsilon = 0.082$ V s^{-1}; $\Delta E = 0.08$ V; $f = 9$ Hz; $R_u = 410$ Ω (a) and 450 Ω (b). Simulation parameters: $D_M = 8.0 \cdot 10^{-6}$ cm^2 s^{-1}; all $\alpha = 0.50$; $K^{SS} = 30$ M^{-1}; $k^{SS}{}_b = 10^{10}$ s^{-1}; $K^{RS} = 0$ M^{-1}; $E^0{}_M = E^0{}_{DII} =$ -1.735 V; (a) $E^0{}_{DI} =$ -1.655 V; $k^0{}_{DI} = 0.017$ cm s^{-1}; $k^0{}_M = 0.15$ cm s^{-1}; $k^0{}_{DII} = 0.02$ cm s^{-1}; (b) $E^0{}_{DI} =$ -1.670 V; $k^0{}_{DI} = 0.02$ cm s^{-1}; $k^0{}_M = 0.055$ cm s^{-1}; $k^0{}_{DII} = 0.014$ cm s^{-1}.

At higher concentrations where "dimer" formation should be more favoured, the departure from the shape expected for an ideal simple one-electron process becomes more pronounced (Fig. 8b). Thus, the FTACV technique demonstrates that the first TIPS-DBC reduction process involves a contribution from both monomeric and "dimeric" units – a conclusion, which was not evident from examination of DC cyclic voltammetric data.

FTACV analysis confirms the substantial concentration dependence of the first oxidation process (Fig. 9), as also detected under conditions of DC cyclic voltammetry.

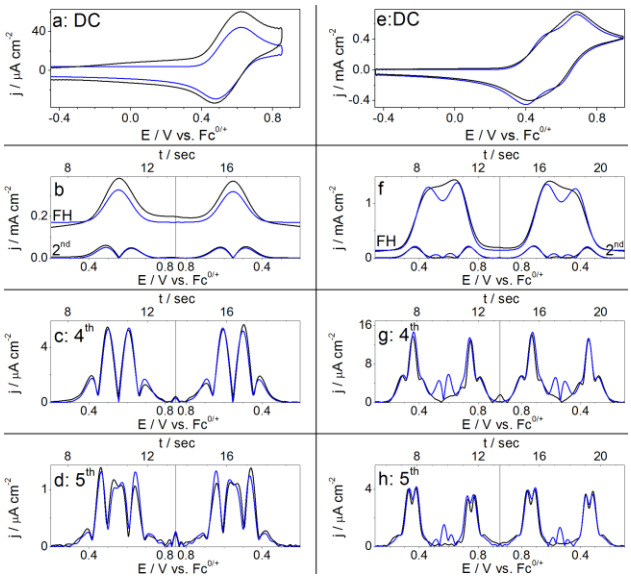

Figure 9. Aperiodic DC (a and e), AC fundamental (FH) and 2nd (b and f), 4th (c and g) and 5th (d and h) harmonic components derived from FTAC voltammograms for oxidation of (a-d) 0.24 and (e-h) 5 mM TIPS-DBC in CH_2Cl_2 (0.2 M (n-Bu)$_4$NPF$_6$) at a GC electrode (*black*) and simulated data (*blue*). Experimental parameters as in Fig. 8 except that υ = 0.104 V s^{-1}. Simulation parameters: D_M = 7.5·10^{-6} cm^2 s^{-1}; all α = 0.5; K^{SS} = 10 M^{-1}; $k^{SS}{}_b = k^{RS}{}_b = 10^{10}$ s^{-1}; (a) K^{RS} = 5102 M^{-1}; $E^0{}_{DI}$ = 0.395 V; $E^0{}_M$ = 0.555 V; $E^0{}_{DII}$ = 0.645 V; $k^0{}_{DI}$ = 0.15 cm s^{-1}; $k^0{}_M$ = 0.10 cm s^{-1}; $k^0{}_{DII}$ = 0.07 cm s^{-1}; (b) K^{RS} = 16393 M^{-1}; $E^0{}_{DI}$ = 0.370 V; $E^0{}_M$ = 0.560 V; $E^0{}_{DII}$ = 0.650 V; $k^0{}_{DI}$ = 0.08 cm s^{-1}; $k^0{}_M$ = 0.025 cm s^{-1}; $k^0{}_{DII}$ = 0.025 cm s^{-1}.

Thus, even at low concentrations, the higher order harmonics have shapes that are substantially different from those predicted for an ideal simple one-electron charge transfer[32] (Fig. 9a). As expected, an increase in the concentration of TIPS-DBC enhances the complexity of the AC harmonic components. In particular, the harmonic components become bifurcated as best seen in the fundamental harmonic (Fig. 9b). The high concentration data imply that at least two processes are present which have different reversible potentials. The simplest explanation is that one process involves oxidation of TIPS-DBC monomers and the other is associated with oxidation of "dimers".

To obtain a quantitative estimate on the influence of the aggregation on reduction and oxidation, simulations of DC and AC cyclic voltammetric curves were undertaken.

Simulations of the DC and AC voltammetric reduction and oxidation of TIPS-DBC. On the basis of mechanisms inferred from the qualitative description of DC and FTAC voltammetry presented above, simulations of the first reduction TIPS-DBC step were undertaken using reaction **I** and the sequence of the processes listed in equations below (where *TD* stands for the monomer and *[TD···TD]* – for the "dimer"; the subscripts *M*, *DI* and *DII* refer to oxidation/reduction of monomer, first and second oxidation/reduction steps of dimer, respectively; Red and Ox refer to reduction and oxidation processes, respectively):

$$TD + e^- \xleftrightarrow{E_M^0(\text{Red}),k_M^0(\text{Red}),\alpha_M(\text{Red})} TD^{\bullet -} \qquad \mathbf{II^{Red}}$$

$$\left[TD\cdots TD\right] + e^- \xleftrightarrow{E_{DI}^0(\text{Red}),k_{DI}^0(\text{Red}),\alpha_{DI}(\text{Red})} \left[TD\cdots TD\right]^{\bullet -} \qquad \mathbf{III^{Red}}$$

$$\left[TD\cdots TD\right]^{\bullet -} + e^- \xleftrightarrow{E_{DII}^0(\text{Red}),k_{DII}^0(\text{Red}),\alpha_{DII}(\text{Red})} \left[TD\cdots TD\right]^{2-} \qquad \mathbf{IV^{Red}}$$

$$TD + TD^{\bullet -} \xleftrightarrow{K^{RS}(\text{Red}),k_f^{RS}(\text{Red})} \left[TD\cdots TD\right]^{\bullet -} \qquad \mathbf{V^{Red}}$$

The first oxidation step was accordingly simulated *via* the mechanism:

$$TD - e^- \xleftrightarrow{E_M^0(\text{Ox}),k_M^0(\text{Ox}),\alpha_M(\text{Ox})} TD^{\bullet +} \qquad \mathbf{II^{Ox}}$$

$$\left[TD\cdots TD\right] - e^- \xleftrightarrow{E_{DI}^0(\text{Ox}),k_{DI}^0(\text{Ox}),\alpha_{DI}(\text{Ox})} \left[TD\cdots TD\right]^{\bullet +} \qquad \mathbf{III^{Ox}}$$

$$\left[TD\cdots TD\right]^{\bullet +} - e^- \xleftrightarrow{E_{DII}^0(\text{Ox}),k_{DII}^0(\text{Ox}),\alpha_{DII}(\text{Ox})} \left[TD\cdots TD\right]^{2+} \qquad \mathbf{IV^{Ox}}$$

$$TD + TD^{\bullet +} \xleftrightarrow{K^{RS}(\text{Ox}),k_f^{RS}(\text{Ox})} \left[TD\cdots TD\right]^{\bullet +} \qquad \mathbf{V^{Ox}}$$

The chemical reversibility observed in the AC and DC cyclic voltammetry for the first reduction and oxidation steps implies products of these transformations are stable on the relevant timescale. The possibility of any significant formation of "dimeric" species as a result of reaction between

radical anions/cations was neglected due to the low probability of interaction of similarly charged species on the basis of electrostatic repulsion considerations and also EPR data. However, these considerations cannot necessarily be used to predict instability of the products of a two-electron reduction or oxidation of a TIPS-DBC "dimer", since, in these cases, the charge can be delocalised in the conjugated π-system associated with the [TIPS-DBC···TIPS-DBC] structure rather than being exclusively localized on each monomeric unit. With respect to inclusion of reactions $\mathbf{V^{Red}}$ and $\mathbf{V^{Ox}}$, there is no obvious reason to reject the possibility of radical-substrate "dimerization", with an equilibrium constant determined by the values of E^0_M, E^0_{DI}, and K^{SS} in accordance with their usual thermodynamic relationships. Simulations including and excluding reaction **V** were therefore undertaken.

The diffusion coefficients of monomers and "dimers" used in the simulations were calculated on the basis of equation 4 and the value of K^{SS} employed in the relevant simulation. Thus, D_M was estimated to be $7.5 \cdot 10^{-6}$ and $9.0 \cdot 10^{-6}$ cm^2 s^{-1} when "dimerization" equilibrium constants of 10 and 100 M^{-1}, respectively, were used in simulation. Initial estimates of E^0 values for reactions $\mathbf{II^{Red}}$ and $\mathbf{II^{Ox}}$ were made on the basis of higher order AC harmonic data derived from solutions with the lowest C_{TD} used in electrochemical studies.

Mechanisms comprising the reaction sequences **I, II^{Red}-IV^{Red}** or **I, II^{Ox}-V^{Ox}** successfully mimic the experimentally observed changes in the DC cyclic voltammetric profiles with variation of C_{TD} (see DC panels in Figs. 8 and 9 and Fig. S4 in Supporting Information) when it is assumed that the formation of the "dimer" facilitates both electrooxidation and electroreduction of TIPS-DBC. However, acceptable agreement of experimental and simulated DC data at the level of confidence exemplified in Fig. S4 can be achieved with other sets of parameters and use of different combinations of reversible potentials for reactions **II-IV**. Obviously, analysis of DC cyclic

voltammograms introduces ambiguity in the E^0 values associated with oxidation and reduction of TIPS-DBC monomers and "dimers". Fortunately, simulations of the higher harmonics derived from FTAC cyclic voltammograms impose considerably stricter constraints and hence provide a more definitive estimation of combinations of E^0 values and rate constants. Figures 8 and 9 provide a comparison of the DC components and higher AC harmonics simulated on the basis of reactions **I**-**V** and experimental data. Clearly, the basic features of the electrochemical data are well captured by the simulations. On the basis of the experiment-simulation comparisons undertaken heuristically, the following conclusions are reached:

a) "Dimerization" of the TIPS-DBC monomers *via* the reactions **I** and **V** occurs at a very fast rate and hence these processes can be assumed to be diffusion controlled (k^f = 10^{10} M^{-1} s^{-1} is assumed).

b) The reversible potential for the reduction of the TIPS-DBC monomer is more negative than that for one-electron reduction of the dimer (reaction $\mathbf{II^{Red}}$**)** by approximately 0.05 V. The E^0 value for the $[TIPS\text{-}DBC\cdots TIPS\text{-}DBC]^{\bullet -/2-}$ process lies between E^0_{DI}*(Red)* and E^0_M*(Red)*, but is close or even equal to the latter value.

c) Interaction between neutral TIPS-DBC monomer and the radical-anion *via* reaction $\mathbf{V^{Red}}$ to yield the "dimeric" structure, which is also the product of reduction process $\mathbf{III^{Red}}$, is unlikely when K^{SS} is less than 50 M^{-1}. When reaction $\mathbf{V^{Red}}$ is excluded, the heterogeneous rate constant for the reduction of the TIPS-DBC monomer is determined to be 0.1-0.2 cm s^{-1}, and hence approximately 5-10 times higher than k^0 for the $[TIPS\text{-}DBC\cdots TIPS\text{-}DBC]^{0/\bullet -/2-}$ processes. At high K^{SS}, the FTACV data can be described by reactions **I** and $\mathbf{II^{Red}}$-$\mathbf{V^{Red}}$ if k^0 for the $[TIPS\text{-}DBC\cdots TIPS\text{-}DBC]^{\bullet -/2-}$ process is assumed to be an order of magnitude higher than for the $TIPS\text{-}DBC^{0/\bullet -}$ and $[TIPS\text{-}DBC\cdots TIPS\text{-}DBC]^{0/\bullet -}$ processes.

d) The E^0 value for the one-electron oxidation of the [TIPS-DBC···TIPS-DBC] "dimer" is less positive than that of the TIPS-DBC$^{0/\bullet+}$ process by at least 0.15 V. The E^0 value for further one-electron oxidation of the dimeric structure is more positive than $E^0_M(Ox)$ by *ca* 0.05-0.10 V.

e) Virtually an equivalent level of agreement of experimental and simulated data for oxidation of TIPS-DBC can be acquired by mechanisms that include or exclude the interaction between neutral and radical-anion monomeric species *via* reaction $\mathbf{V^{Ox}}$. In the former case, a good fit can be achieved using low K^{SS} values, which are consistent with the ^{1}H NMR estimate, while the scheme excluding process $\mathbf{V^{Ox}}$ requires the TIPS-DBC dimerization equilibrium constant to be higher (30-50 M^{-1}). The magnitudes of k^0 values for oxidation of TIPS-DBC monomers and dimers are all comparatively large (0.05 - 0.15 cm s^{-1}), although $k^0_{DI}(Ox)$ (reaction $\mathbf{III^{Ox}}$) is predicted to be higher than for processes $\mathbf{II^{Ox}}$ and $\mathbf{IV^{Ox}}$.

The E^0 values for reactions **II-IV** extracted by simulation using the K^{SS} equilibrium constant value estimated from ^{1}H NMR and microelectrode measurements are consistent with EPR data acquired after oxidation of 1 mM TIPS-DBC. With these thermodynamic parameters, the TIPS-DBC$^{\bullet+}$ radical cation detected by EPR spectroscopy after oxidation of a 1 mM solution of TIPS-DBC is predicted to be the dominant species at a concentration above 0.85 mM along with a small contribution from the [TIPS-DBC···TIPS-DBC]$^{2+}$ dimer dication. An analogous situation applies to the EPR analysis of the 1 mM TIPS-DBC solution subjected to one-electron bulk reductive electrolysis, where the anion radical is predicted to be the dominant species present.

Simulations based on reaction sequences **I-V** satisfactorily describe the key features of oxidation and reductions of TIPS-DBC, although whether a unique solution has been derived is always questionable when all processes are very fast and the system equilibrates rapidly. More extensive aggregation is in principle possible, but not considered, as agreement between theory and

experiment over the concentration range studied was satisfactory. Importantly, the analysis unequivocally reveals that the formation of the TIPS-DBC "dimer" facilitates one-electron oxidation and reduction, *i.e.* shifts the E^0(Ox) and E^0(Red) reversible potentials to less and more positive values, respectively.

Concentration dependence of HOMO and LUMO energy levels. Although some uncertainty in correlation of the individual HOMO/LUMO levels calculated on the basis of solution phase voltammetric measurements to the vacuum scale exists,[13] quantitative comparisons of the changes of energy levels acquired from voltammetric data are valid.

The estimated value of potential corresponding to the onset of reduction of TIPS-DBS dissolved in dichloromethane *ca* -1.66 V is independent of C_{TD} under DC voltammetric conditions. In contrast, the oxidation onset potential ($E_{Ox\text{-}onset}$) decreases gradually on increasing the concentration of TIPS-DBC as summarized in Table 1. The change of HOMO level induced by an increase in TIPS-DBC concentration from 0.24 to 10 mM (Table 1) is comparable to the difference of 0.08 ± 0.2 eV reported for TIPS-DBC films having pronouncedly distinct mictrostructure.[15] In this sense, the voltammetric analysis supports the proposed crucial role of intermolecular association of TIPS-DBC molecules occurring in the solution and further transposed to the morphology of the solid film donor layer on the performance of the OPV device. As demonstrated recently in,[15] the contribution of the TIPS-DBC molecular aggregation to the V_{oc} value can be efficiently controlled by the organic semiconductor deposition procedure.

Table 1. HOMO energy level of TIPS-DBC estimated from the potential of the onset of oxidation detected by cyclic voltammetry ($E_{Ox\text{-}onset}$) as a function of total concentration.

C_{TD} / mM	$E_{Ox\text{-}onset}$ / V	HOMO / eV [a]
0.24	0.46	-5.26

1.0	0.41	-5.20
2.0	0.38	-5.18
5.0	0.35	-5.15
10	0.32	-5.12

[a] Calculated using -4.8 eV as the value for the $Fc^{0/+}$ half-cell reaction.

CONCLUSIONS

A detailed electrochemical and spectroscopic study of TIPS-DBC in dichloromethane has revealed that molecular aggregation, presumably *via* π-π stacking, contributes to the redox chemistry and energy levels of this organic semiconductor, which is an efficient donor material for OPVs.[14,15] Using the assumption of aggregation of TIPS-DBC as π-π stacked "dimer", an equilibrium constant in the range 10-150 M^{-1} was estimated on the basis of analysis of ^{1}H NMR and near steady-state voltammetric data.

As shown by EPR spectroscopy, the one-electron reduction and oxidation of TIPS-DBC produces essentially monomeric radical cations and anions, respectively, under concentration conditions where significant aggregation of the parent molecule does not occur. An increase in concentration induces large changes in the DC voltammetric oxidation of TIPS-DBC, while the reductive behaviour remains similar to that expected for a simple one-electron process. The concentration dependent patterns of behaviour found in the highly sensitive FTAC voltammetric technique confirm that both reduction and oxidation of TIPS-DBC in dichloromethane involve monomers and aggregates. Although aggregation might not be strictly limited to "dimerization" in the concentration range used in the present work, reaction sequences simulated on the basis of only monomeric and "dimeric" units satisfactorily mimic the key features of the oxidation and reduction

processes and provide estimates of the electrode kinetics and E^0 values. Importantly, FTACV data unequivocally reveals that aggregation facilitates both oxidation and reduction of TIPS-DBC by shifting the reversible potentials to less and more positive values, respectively. Postulated changes in the TIPS-DBC redox chemistry induced by intermolecular association in solution correlate with the performance of the OPVs that utilize TIPS-DBC donor solid films with different degrees of aggregation.[15]

The finding of aggregation in dichloromethane provides data and insights needed for characterisation of the performance of organic semiconductors, and the voltammetric behaviour represents an example of an unusual mechanism that has not been well documented to date.

ACKNOWLEDGMENTS

The authors express their appreciation to Dr. R. Mulder from CSIRO for performing the ^{1}H NMR analysis and to Prof. R. T. Boeré from University of Lethbridge for valuable discussion on the interpretation of the EPR data. This research was funded through the Flexible Electronics Theme of the CSIRO Future Manufacturing Flagship and was also supported by the Victorian Organic Solar Cell Consortium (Victorian Department of Primary Industries, Sustainable Energy Research and Development Grant; Victorian Department of Business and Innovation, Victoria's Science Agenda Grant; and the Australian Renewable Energy Agency) and the Australian Centre for Advanced Photovolatics (ACAP). Financial support from the Australian Research Council under Discovery Project No. 120101470 also is gratefully acknowledged.

ASSOCIATED CONTENT

Supporting Information. Experimental details for voltammetric, HPLC, NMR, EPR and UV-Vis-NIR characterization. Algebraic manipulations required for estimation of K^{SS} from NMR

and near steady-state voltammetric data. Fig. S1 showing HPLC data for TIPS-DBC and structures of identified impurities. Table S1 listing details of theoretically calculated allowed singlet transitions for TIPS-DBC. Figs. S2 and S3 showing EPR spectra generated from oxidation of TIPS-DBC. Table S2 listing parameters used for the simulation of EPR spectra. Fig. S4 comparing simulated and experimental DC voltammograms for oxidation of TIPS-DBC. This information is available free of charge *via* the Internet at http://pubs.acs.org.

AUTHOR INFORMATION

Corresponding Authors

Alexandr.Simonov@monash.edu, +61 3 9905 1520 (A.N.S.), Scott.Watkins@csiro.au, +61 3 9545 2618 (S.E.W.), Alan.Bond@monash.edu, +61 3 9905 1338 (A.M.B.)

Present address

Pozo-Gonsalo, C.: ARC Centre of Excellence for Electromaterials Science, IFM-Institute for Frontier Materials, Deakin University, 221 Burwood Hwy, Burwood, Victoria 3125, Australia

Attia, A.: Department of Physical Chemistry, National Research Centre, El Buhouth St., 12311, Dokki, Cairo, Egypt.

Nafady, A.: Department of Chemistry, College of Science, King Saud University, PO Box: 2455, Riyadh – 11451, Saudi Arabia

REFERENCES

(1) Sariciftci, N. S.; Smilowitz, L.; Heeger, A. J.; Wudl, F. Photoinduced Electron Transfer from a Conducting Polymer to Buckminsterfullerene. *Science* **1992**, *258*, 1474-1476.

(2) Mishra, A.; Bäuerle, P. Small Molecule Organic Semiconductors on the Move: Promises for Future Solar Energy Technology. *Angew. Chem. Int. Ed.* **2012**, *51*, 2020–2067.

(3) Sun, Y.; Welch, G. C.; Leong, W. L.; Takacs, C. J.; Bazan, G. C.; Heeger, A. J. Solution-Processed Small-Molecule Solar Cells with 6.7% Efficiency. *Nature Mater.* **2012**, *11*, 44–48.

(4) Rand, B. P.; Burk, D. P.; Forrest, S. R. Offset Energies at Organic Semiconductor Heterojunctions and their Influence on the Open-Circuit Voltage of Thin-Film Solar Cells. *Phys. Rev. B* **2007**, *75*, 115327.

(5) Scharber, M. C.; Muhlbacher, D.; Koppe, M.; Denk, P.; Waldauf, C.; Heeger, A. J.; Brabec, C. L. Design Rules for Donors in Bulk-Heterojunction Solar Cells - Towards 10 % Energy-Conversion Efficiency. *Adv. Mater.* **2006**, *18*, 789–794.

(6) Vandewal, K.; Gadisa, A.; Oosterbaan, W. D.; Bertho, S.; Banishoeib, F.; Van Severen, I.; Lutsen, L.; Cleij, T. J.; Vanderzande, D.; V., Manca, J. V. The Relation Between Open-Circuit Voltage and the Onset of Photocurrent Generation by Charge-Transfer Absorption in Polymer : Fullerene Bulk Heterojunction Solar Cells. *Adv. Funct. Mater.* **2008**, *18*, 2064–2070.

(7) Perez, M. D.; Borek, C.; Forrest, S. R.; Thompson, M. E. Molecular and Morphological Influences on the Open Circuit Voltages of Organic Photovoltaic Devices. *J. Am. Chem. Soc.* **2009**, *131*, 9281-9286.

(8) Hwang, J.; Wan, A.; Kahn, A. Energetics of Metal–Organic Interfaces: New Experiments and Assessment of the Field. *Mater. Sci. Eng. R* **2009**, *64*, 1–31.

(9) D'Andrade, B. W.; Datta, S.; Forrest, S. R.; Djurovich, P.; Polikarpov, E.; Thompson, M. E. Relationship Between the Ionization and Oxidation Potentials of Molecular Organic Semiconductors. *Org. Electronics* **2005**, *6*, 11–20.

(10) Davis, R. J.; Lloyd, M. T.; Ferreira, S. R.; Bruzek, M. J.; Watkins, S. E.; Lindell, L.; Sehati, P.; Fahlman, M.; Anthony, J. E.; Hsu, J. W. P. Determination of Energy Level Alignment at

Interfaces of Hybrid and Organic Solar Cells Under Ambient Environment. *J. Mater. Chem* **2011**, *21*, 1721-1729.

(11) Djurovich, P. I.; Mayo, E. I.; Forrest, S. R.; Thompson, M. E. Measurement of the Lowest Unoccupied Molecular Orbital Energies of Molecular Organic Semiconductors. *Org Electronics* **2009**, *10*, 515–520.

(12) Johansson, T.; Mammo, W.; Svensson, M.; Andersson, M. R.; Inganas, O. Electrochemical Bandgaps of Substituted Polythiophenes. *J. Mater. Chem* **2003**, *13*, 1316–1323.

(13) Cardona, C. M.; Li, W.; Kaifer, A. E.; Stockdale, D.; Bazan, G. C. Electrochemical Considerations for Determining Absolute Frontier Orbital Energy Levels of Conjugated Polymers for Solar Cell Applications. *Adv. Mater.* **2011**, *23*, 2367-2371.

(14) Winzenberg, K. N.; Kemppinen, P.; Fanchini, G.; Bown, M.; Collis, G. E.; Forsyth, C.M.; Hegedus, K.; Singh, Th. B.; Watkins, S. E. Dibenzo[b,def]chrysene Derivatives: Solution-Processable Small Molecules that Deliver High Power-Conversion Efficiencies in Bulk Heterojunction Solar Cells. *Chem. Mater.* **2009**, *21*, 5701–5703.

(15) Scholes, F. H.; Ehlig, T.; James, M.; Lee, K. H.; Duffy, N.; Scully, A. D.; Singh, T. B.; Winzenberg, K. N.; Kemppinen, P.; Watkins, S. E. Intraphase Microstructure – Understanding the Impact on Organic Solar Cell Performance. *Adv. Funct. Mater.* **2013**, DOI: 10.1002/adfm.201300726.

(16) Bond, A. M.; Duffy, N. W.; Guo, S.-X.; Zhang, J.; Elton, D. Changing the Look of Voltammetry: Can FT Revolutionize Voltammetric Techniques as it Did for NMR?. *Anal. Chem.* **2005**, *77*, 186A-195A.

(17) Nafady, A.; Costa, P. J.; Calhorda, M. J.; Geiger, W. E. Electrochemical Oxidation of CoCp(CO)2: Radical-Substrate Reaction of a 17e-/18e- Pair and Production of a Unique Dimer Radical. *J. Am. Chem. Soc.* **2006**, *128*, 16587-16599.

(18) http://www.elchsoft.com.

(19) http://www.garethkennedy.net/MECSim.html.

(20) Frisch, M. J.; Trucks, G. W.; Schlegel, H. B.; Scuseria, G. E.; Robb, M. A.; Cheeseman, J. R.; Scalmani, G.; Barone, V.; Mennucci, B.; Petersson, G. A. et al. Gaussian 09, Revision B.01; Gaussian, Inc., Wallingford, CT, 2010.

(21) Burke, K. B.; Shu, Y.; Kemppinen, P.; Singh, B.; Bown, M.; Liaw, I. I.; Williamson, R. M.; Thomsen, L.; Dastoor, P.; Belcher, W. et al. Single Crystal X-ray, AFM, NEXAFS, and OFET Studies on Angular Polycyclic Aromatic Silyl-Capped 7,14-Bis(ethynyl)dibenzo[b,def]chrysenes. *Cryst. Growth Des.* **2012**, *12*, 725−731.

(22) Fielding, L. Determination of Association Constants (Ka) from Solution NMR Data. *Tetrahedron* **2000**, *56*, 6151-6170.

(23) Turcu, I.; Bogdan, M. Size Dependence of Molecular Self-Assembling in Stacked Aggregates. 1. NMR Investigation of Ciprofloxacin Self-Association. *J. Phys. Chem. B* **2012**, 116, 6488−6498.

(24) Chen, Z.; Lohr, A.; Saha-Moller, C. R.; Wurthner, F. Self-Assembled π-Stacks of Functional Dyes in Solution: Structural and Thermodynamic Features. *Chem. Soc. Rev.* **2009**, *38*, 564-584.

(25) Nakano, M.; Nakano, N. I.; Higuchi, T. Calculation of Stability Constants of Hydrogen-Bonded Complexes from Proton Magnetic Resonance Data. Interactions of Phenol with Dimethylacetamide and Various Ketones. Solvent Effect. *J. Phys. Chem.* **1967**, *71*, 3954-3959.

(26) Geiger, W. E.; Barrière, F. Organometallic Electrochemistry Based on Electrolytes Containing Weakly-Coordinating Fluoroarylborate Anions. *Accounts Chem. Res.* **2010**, *43*, 1030-1039.

(27) Gooding, J. J.; Compton, R. G.; Brennan, C. M.; Atherton, J. H. A New Electrochemical Method for the Investigation of the Aggregation of Dyes in Solution. *Electroanalysis* **1997**, *9*, 759-764.

(28) Boulas, P. L.; Gomez-Kaifer, M.; Echegoyen, L. Electrochemistry of Supramolecular Systems. *Angew. Chem. Int. Ed.* **1998**, *37*, 216-247.

(29) Kuroiwa, Y.; Kato, Y.; Watanabe, T. Negative shift of chlorophyllaoxidation potential by aggregation in acetonitrile/ionic liquid mixed solvents. *J. Photochem. Photobiol. A.* **2009**, *202*, 191–195.

(30) Blois, M. S., Jr.; Brown, H. W.; Maling, J. E. In *Free Radicals in Biological Systems*; Blois, M. S., Jr.; Brown, H. W.; Lemmon, R. M.; Lindblom, R. O.; Weissbluth, M., Eds.; Academic Press: New York and London, 1961; p. 117.

(31) Bond, A. M.; Mashkina, E. A.; Simonov, A. N. In *Developments in Electrochemistry*; Pletcher, D.; Tian, Z.-Q.; Williams, D. E. Eds.; John Wiley & Sons, Ltd.: United Kingdom, 2014; pp. 21-47.

(32) Bullock, J. P.; Mashkina, E.; Bond, A. M. Activation Parameters Derived From a Temperature Dependent Large Amplitude ac Voltammetric Study of the Electrode Kinetics of the $Cp_2M^{0/+}$ Redox Couples (M = Fe, Co) at a Glassy Carbon Electrode. *J. Phys. Chem. A* **2011**, *115*, 6493–6502.

For TOC only

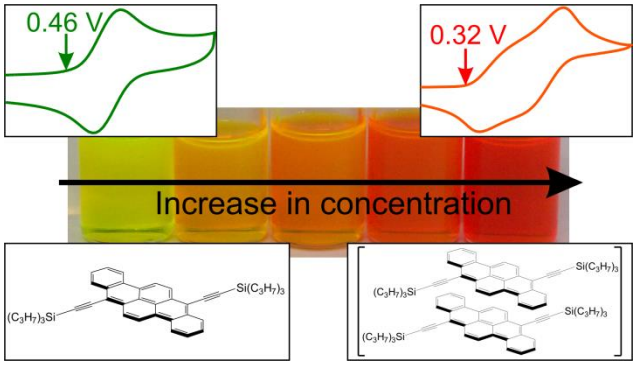
0.46 V
0.32 V
Increase in concentration
Si(C3H7)3
(C3H7)3Si
Si(C3H7)3
(C3H7)3Si
Si(C3H7)3
(C3H7)3Si